Available online at www.sciencedirect.com
SCIENCE DIRECT®
Chemistry and Physics of Lipids 135 (2005) 83–92
CPL
CHEMISTRY AND PHYSICS OF LIPIDS
www.elsevier.com/locate/chemphyslip

Phase transitions in crystals of racemic long chain 2-amino alcohols

Pantelis Xynogalas [a], Athanasios Kanapitsas [b], Violetta Constantinou-Kokotou [c], Polycarpos Pissis [b], Kyriakos Viras [a,*]

[a] *National and Kapodistrian University of Athens, Chemistry Department, Laboratory of Physical Chemistry, Panepistimiopolis, Athens 157 71, Greece*
[b] *National Technical University of Athens, Physics Department, Zographou Campus, Athens 157 80, Greece*
[c] *Chemical Laboratories, Agricultural University of Athens, Athens 118 55, Greece*

Received 19 May 2004; accepted 3 February 2005
Available online 8 March 2005

Abstract

Various techniques, namely differential scanning calorimetry, optical microscopy, dielectric and Raman spectroscopy, all covering a wide range of temperatures, were used to study the thermodynamically stable phases and molecular mobility of crystals of long chain 2-amino alcohols. The results showed that two different crystal forms are present in each sample. The temperature behaviour of the phases is studied in details.

Keywords: 2-Amino alcohols; Polymorphism; LAM modes; Rotator phase

1. Introduction

Many long chain crystalline compounds exhibit polymorphism (Wunderlich, 1990; Sprunt et al., 2000), meaning that, depending upon the given processing conditions, the crystalline form may exist in two or more states or modifications. Usually, the crystalline states exhibit different levels of thermodynamic stability with an unstable form melting at a temperature significantly lower than the melting point of the thermodynamically stable form. Depending upon the conditions used to generate the crystalline state(s), the molecular crystal may exhibit one or more thermodynamically stable and unstable polymorphic crystalline states. In addition to that during heating while one state undergoes melting, subsequently the same state may be followed by crystallisation, and then melting at higher temperatures, due to the formation of a more stable state. The polymorphic behaviour observed in several long chain compounds, i.e., alka-

* Corresponding author. Tel.: +30 210 7274571; fax: +30 210 7274752.
E-mail address: viras@chem.uoa.gr (K. Viras).

0009-3084/$ – see front matter © 2005 Elsevier Ireland Ltd. All rights reserved.
doi:10.1016/j.chemphyslip.2005.02.007

nes, normal fatty acids, amino acids, etc., is generally characterised by higher structural variations caused by differences in the stacking modes of molecular layers (Kobayashi et al., 1980, 1984; Boistelle et al., 1976; Amelinckx, 1955; Kaneko et al., 1994; Nagle, 1980).

Saturated and unsaturated long chain 2-amino alcohols, which may be considered as sphingosine analogues, are of special interest because they display various biological activities (Constantinou-Kokotou, 2002). They exhibit cytotoxic activity against various cancer cell lines (Markidis et al., 2001) and induce apoptosis through a caspace-3 dependent pathway (Del Olmo et al., 2002). In addition, they present in vivo anti-inflammatory activity (Kokotos et al., 1999; Magrioti et al., 2003) and immunosuppressant activity (Hirose et al., 1996).

This work presents detailed studies on the solid phase behaviour of 2-amino alcohols with 14, 16 and 18 carbon atoms. These crystalline materials pass mainly through three stable modifications between room temperature and their melting points. A variety of experimental techniques as differential scanning calorimetry (DSC), optical microscopy (OM), dielectric spectroscopy (DS) and Raman spectroscopy (RS) were applied in order to characterise in detail the molecular motions and different forms in the three solid phases with the general aim of gaining a better understanding of phase transitions in 2-amino alcohols.

2. Materials and methods

2.1. Materials

Hydrochloride salts of racemic 2-amino-tetradecanol, 2-amino-hexadecanol and 2-amino-octadecanol were prepared as described in literature (Kokotos et al., 1992). The hydrochloride salt of (*S*)-2-amino-hexadecanol was prepared by deprotection of (*S*)-2-(*tert*-butoxycarbonylamino)-hexadecanol (Kokotos et al., 1996).

2.2. Differential scanning calorimetry

Perkin-Elmer DSC-4 was used. Known weights (5–10 mg) of dry samples stored either at room temperature or in a freezer at $-10\,^{\circ}C$ were sealed into aluminum pans under nitrogen in a dry box. Samples were usually heated at $5\,^{\circ}C\,min^{-1}$. DSC curves were analysed using the data station of the DSC-4. Values of the enthalpy of transition, ΔH_{tr}, were obtained from peak areas (usually to $\pm 5\,J\,mol^{-1}$) and transition temperatures were obtained from positions of peak maxima or minima (usually to $\pm 1\,^{\circ}C$). The power and temperature scales of the calorimeter were calibrated against the enthalpies of fusion and melting temperature of pure indium, and the temperature scale was checked against the melting points of organic standards covering the temperature range of interest. Correction for thermal lag was based on examination of certain standards at different heating rates and extrapolation to zero heating rate via plots of T_m against root heating rate. Thermal treatment was carried out in the instrument by successive constant rate heating–cooling cycles.

2.3. Optical microscopy

A Leitz optical polar microscope was used connected with a Mettler F82 heating plate and a programmer of Linkam TMS91. Micrographs at different temperatures were taken with a Wild MPS 51S camera suitable fitted on the polar microscope.

2.4. Dielectric spectroscopy

For dielectric measurements the material was pressed in a stainless steel die at about 8–10 t to a pellet of 13 nm diameter and about 1mm thickness. The pellet was clamped between Au-plated stainless steel electrodes and inserted into a Novocontrol cryostat. The dielectric properties were measured in the broad frequency range of 10^{-2} to 10^{6} Hz by means of the Schlumberger frequency response analyser FRA SI-1260 and a Hewlett-Packard LCR meter HP-4284A. Measurements were performed isothermally at several temperatures (temperature stability better than $\pm 0.1\,^{\circ}C$) in the range 30–100 °C using the Quatro Cryosystem of Novocontrol. The sample was kept at each temperature for about 30 min (about 20 min for temperature stabilisation and about 10 min for frequency sweep).

2.5. Raman spectroscopy

Low-frequency Raman spectra were recorded with a Spex Ramalog spectrometer fitted with a 1403 double monochromator, with a third (1442U) monochromator operated in scanning mode. The light source was a Coherent Innova 90 argon-ion laser operated at 514.5 nm. The scattered radiation was collected at an angle of 90° to the incident beam. Spectra were recorded at a laser power of 300 mW at sample with a resolution of 1 cm^{-1}. The low-frequency scale was calibrated with reference to the 9.6 and 14.9 cm^{-1} bands of the low-frequency spectrum of L-cystine. Baseline corrections were applied as required.

High-frequency Raman spectra were recorded with a Perkin-Elmer GX Fourier transform spectrometer. A diode pumped Nd:YAG laser at 1064 nm was used as the excitation source. The scattered radiation was collected at an angle of 180° to the incident beam. Spectra were recorded at a laser power of 300 mW at sample with a resolution of 2 cm^{-1}. In order to obtain a good signal to noise ratio, typically, 2000 scans were co-added for the spectra. The temperature dependence of the Raman spectra was taken using the temperature accessory from Ventacon (stability ±0.5 °C). Analysis of the spectra was carried out using GRAMS/32 data analysis software.

3. Results and discussion

3.1. Thermal analysis

A number of phases were revealed after slow recrystallisation of 2-amino alcohols. Several constant rate heating/cooling cycles it was required in order to obtain thermodynamically stable phases. These phases gave three main crystalline modifications, appearing during the heating process before the melting point of each sample had been reached. The different phases of 2-amino alcohols are shown in Figs. 1–3. As indicated in Figs. 1c and 2, the first crystalline form melts at 50.5 °C and 23.9 °C for 2-amino-hexadecanol and 2-amino-tetradecanol, respectively. A second phase, the so-called rotator phase is followed at about 88.2 °C, for 2-amino-tetradecanol, and finally, by the melting point of the second crystalline form at 98.2 and 95.9 °C for 2-amino-hexadecanol and 2-amino-tetradecanol, respectively. At the rotator phase, the chains should rotate quasi-freely about their long axes (Ungar, 1983; Denicolo et al., 1983). The exotherm at 79.7 °C (Fig. 1c) in-

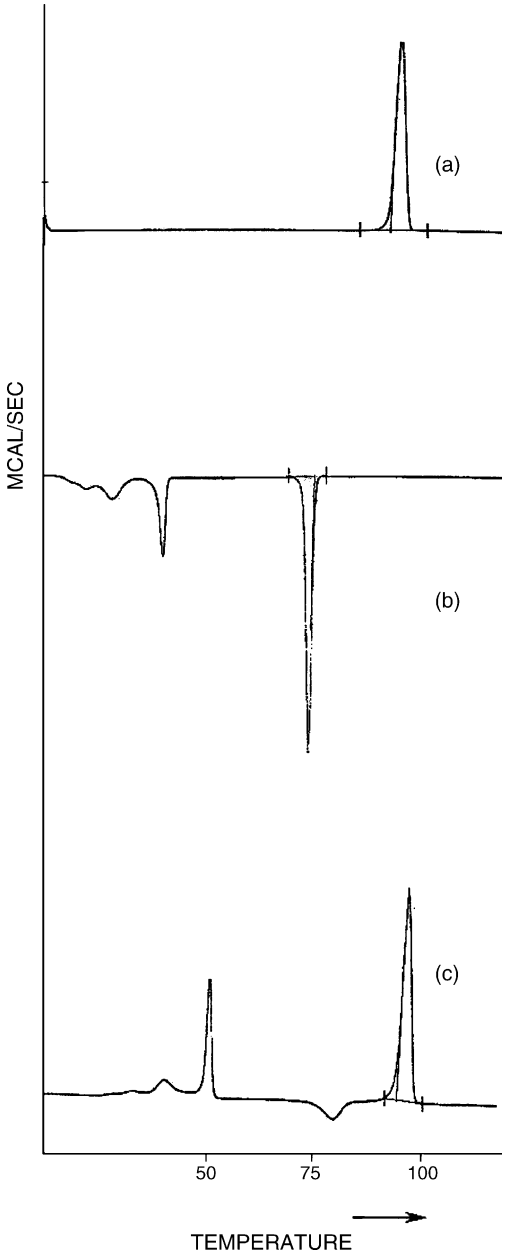

Fig. 1. DSC curves for sample 2-amino-hexadecanol: (a) first heating at 5 °C min^{-1} and (b and c) subsequently cooling and heating at the same rate.

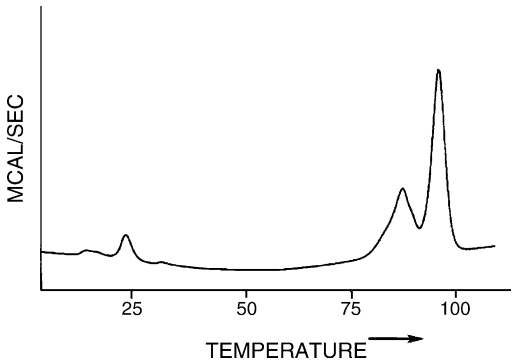

Fig. 2. DSC curve for sample 2-amino-tetradecanol heated at 5 °C min^{-1}.

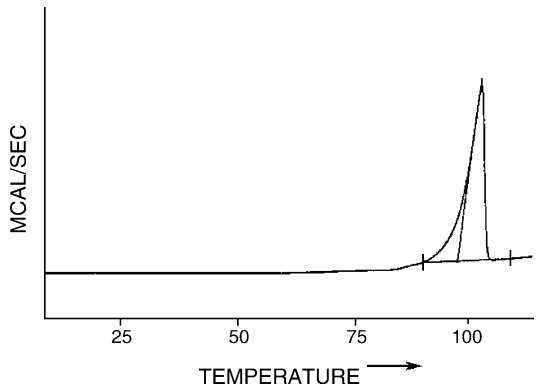

Fig. 3. DSC curve for sample (*S*)-enantiomer of 2-amino-hexadecanol heated at 5 °C min^{-1}.

dicates a re-organisation of the sample before the melting point of the racemic compound.

Temperatures and transition heat values of the observed main phases of long chain 2-amino alcohols are listed in Table 1.

The rotator phase of 2-amino-octadecanol has been observed only during the cooling process. The (*S*)-enantiomer of 2-amino-hexadecanol also studied, displayed only one crystalline structure, with a melting point at 103.1 °C, a slightly higher temperature than the melting point of the corresponding racemic compound (Fig. 3).

The extensive supercooling effect of samples (Table 1) during crystallisation can be explained by the formation of relatively large crystals, as confirmed by the micrographs of optical microscopy.

3.2. Optical microscopy

Optical microscopy was used in order to confirm the thermal analysis results. In Fig. 4, the micrograph of 2-amino-hexadecanol at 60 °C is shown. The first crystalline form of the sample is in the melt state, while crystals of the second crystalline form are clearly observed.

3.3. Dielectric spectroscopy

The basis for using dielectric spectroscopy in phase transition studies is that the dielectric properties are, in general, different in the various phases of a material. The main advantage of dielectric spectroscopy for such studies, as compared to other techniques, is that the broad frequency range covered may provide significant information on the structure and morphology of the various phases. Thus, in addition to its wide use for glass transition studies in liquids and polymers (Donth, 2001), dielectric spectroscopy is often used for melting and crystallisation studies in polymers (Mijovic and Sy, 2002) and liquid crystalline polymers (Nikonorova et al., 2003).

Fig. 5 shows the temperature dependence of the dielectric constant ε' (real part) of 2-amino-tetradecanol. The data have been recorded isothermally as described above and have been re-plotted here. The data are compared with those of thermal analysis (Fig. 2). A high

Table 1
Temperatures and transition heat values of the observed main phases of 2-amino alcohols

n	T_m/T_c (°C) (first phase); $\Delta H_m/\Delta H_c$ (kJ mol^{-1})	T_{rot} (°C) (rotator phase); ΔH_{rot} (kJ mol^{-1})	T_m/T_c (°C) $\Delta H_m/\Delta H_c$ (kJ mol^{-1})
14	23.9/15.6; 3.32/3.29	88.2; 5.20	95.9/71.3; 16.93/16.05
16	50.5/39.2; 9.85/9.65	95.6; 5.65	98.2/73.2; 27.54/26.62
S-16		91.3; 5.18	103.1/78.8; 29.30/30.00
18	65.8/56.0; 11.22/11.78		107.8/62.5; 33.45/32.12

n, number of carbon chain atoms. T_m, T_c, T_{rot}, ΔH_m, ΔH_c and ΔH_{rot} are phase transition temperatures and enthalpies, of melting, crystallisation and rotator phase, respectively.

Fig. 4. Optical microscopy micrograph for sample 2-amino-hexadecanol at 60 °C.

frequency (10^4 Hz) has been chosen to eliminate conductivity and space charge polarisation effects dominating the lower frequencies (Kremer and Schoenhals, 2002). Comparing with other techniques two points have to be taken into account: (a) the different thermal treatment of the sample, as described in the experimental part, and (b) the fact that the sample was not sealed during dielectric measurements but rather exposed to environment. The temperature independent and rather low value of ε' (a good measure of molecular mobility (Kremer and Schoenhals, 2002)) up to about 50 °C is characteristic of crystal structures of stiff molecules. Molecular mobility increases at higher temperatures and the broad shape maximum at about 75 °C indicates a phase transition. The steep increase and the high values of ε' at $T \geq 90$ °C suggest a significant increase of molecular mobility, which should be attributed to loosening of crystal and/or molecular structure. Fig. 6 refers to the temperature dependence of electrical conductivity σ obtained from the dielectric measurements. O_{dc} is temperature independent and low at $T \leq 50$ °C, providing support for rigid structure at low temperatures. The significant increase at temperatures between 50 and 75 °C indicates a phase transition in this region, which is consistent with the fact that σ_{dc} and σ_{ac} coincide at $T \geq 75$ °C, whereas they deviate at lower temperatures. The temperature dependence of σ in the range 75–90 °C is characteristic for a stable phase, whereas the significant increase at $T \geq 90$ °C suggests loosening

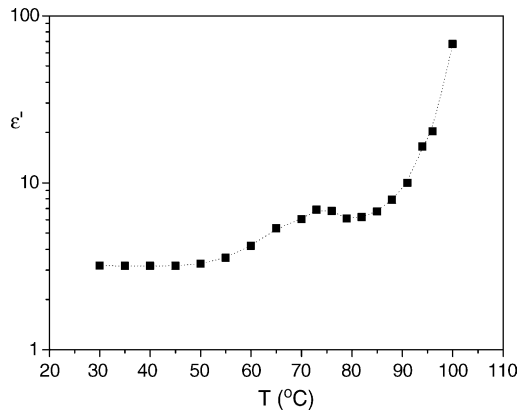

Fig. 5. Temperature dependence of dielectric constant ε' in 2-amino-tetradecanol at a constant frequency of 10^4 Hz.

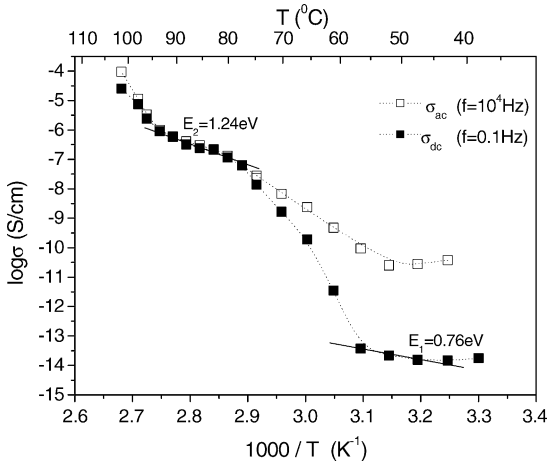

Fig. 6. Temperature dependence of electrical conductivity σ in 2-amino-tetradecanol at $f = 10^4$ and 0.1 Hz.

of the structure, in agreement with the data in Fig. 5. The Arrhenius equation

$$\sigma_{dc}(T) = A \exp\left(\frac{-E}{kT}\right)$$

where E is the activation energy, k the Boltzmann's constant and A is a pre-factor, has been fitted to the σ_{dc} data. The results (not shown here) give $E = 0.76$ eV at $T \leq 50\,^{\circ}$C and $E = 1.24$ eV at $75\,^{\circ}\text{C} \leq T \leq 90\,^{\circ}$C, suggesting stable phases in these temperature regions, a phase transition between 50 and 75 °C and loosening of the structure at $T \geq 90\,^{\circ}$C.

Summarising, the dielectric data suggest a rigid phase at $T \leq 50\,^{\circ}$C and a gradual loosening of the crystal structure in the temperature range 50–75 °C, which is completed at about 75 °C (under the conditions of dielectric measurements). In the temperature range 75–90 °C, the sample is in the rotator phase. The slight decrease of $\varepsilon'(T)$ in this region in Fig. 5, is in agreement with a loose coupling of molecular dipoles described by the Langevin equation, $\varepsilon'(T) \sim 1/T$. Finally, the significant increase in $\varepsilon'(T)$ and $\sigma(T)$ at $T \geq 90\,^{\circ}$C must be attributed to the transition from the rotator to melt, not yet completed in the temperature range of measurements in Figs. 5 and 6. Measurements at higher temperatures should be less reliable because of changes in the geometrical dimensions of the sample.

3.4. Raman spectroscopy

3.4.1. Low-frequency spectra—LAM modes

Raman spectroscopy is a convenient tool for studying low-frequency modes that are sensitive to the molecular aggregation states of long chain compounds (Snyder et al., 1994). Since the frequencies and profiles of the Raman bands reflect, sensitively, intermolecular forces, we are able to obtain various structural information including the lateral packing of molecules, layer stacking as polymorphism and molecular motions. Among these modes, the one node longitudinal acoustic mode (LAM-1) has been used for the determination of chain morphology in lamellar crystals of long chain molecules (Viras et al., 1989; Campbell et al., 1991; Soutzidou et al., 1999, 2002). Low-frequency Raman spectra (5–250 cm^{-1}) for 2-amino alcohols are shown in Fig. 7.

In our previous paper (Soutzidou et al., 2002), we studied the low-frequency Raman bands of *n*-alcohols, where the frequencies of the LAMs were interpreted in terms of the linear crystal model of Minoni and Zerbi (1982), by taking in account the perturbation of the LAM frequencies by end effects.

Wave profiles calculated for the first two longitudinal modes of the H-bonded dimer led us to the notation of LAM-1 and LAM-3 modes, of the dimer and the unimer, respectively. LAM-1 and LAM-3 band frequencies of 2-amino alcohols (Table 2) are almost identical to those of *n*-alcohols, of same chain length. The observed slightly difference in frequencies of 2-amino alcohols is attributed to the presence of NH_3^+ ion. Furthermore, the similarities of high and low-frequency spectra for 2-amino alcohols and the corresponding *n*-alcohols, lead to the conclusion that the structure of both compounds is almost the same (Soutzidou et al., 2002).

An important aspect associated with the LAM bands is the splitting effect observed in 2-amino alcohols. This splitting is related to the polymorphic structure of the samples, and has been found in a higher order structural variation in several long chain molecules (Fig. 8).

3.4.2. High frequency spectra—Temperature dependence

High frequency Raman spectra of 2-amino-hexadecanol at different temperatures are shown in Fig. 9. The temperature dependence of the confor-

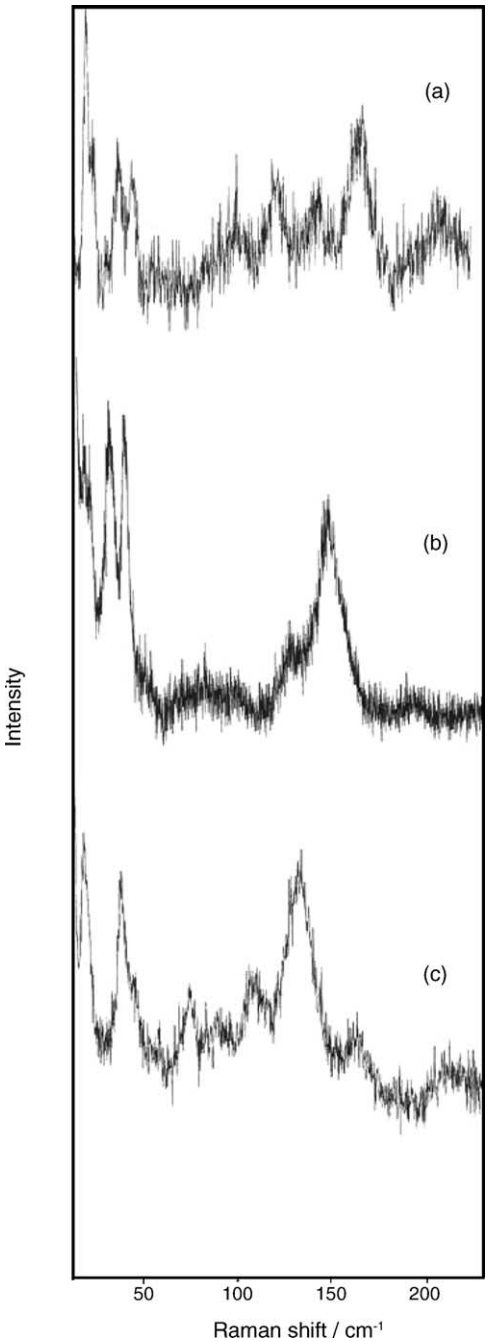

Fig. 7. Low-frequency Raman spectra of: (a) 2-amino-tetradecanol; (b) 2-amino-hexadecanol; (c) 2-amino-octadecanol.

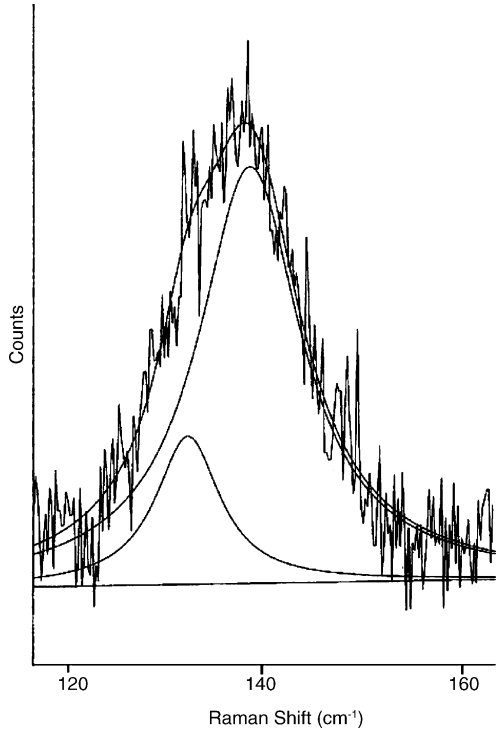

Fig. 8. An example of a Lorentzian–Gaussian deconvoluted Raman spectrum of 2-amino-hexadecanol.

mationally sensitive bands in the C–H stretching region (2800–3100 cm^{-1}) was used to estimate the alterations in intrachain *trans*/*gauche* conformation and chain packing properties (Huang and Levin, 1983; O'Leary et al., 1984).

In order to quantify this effect, the temperature dependence of the peak height intensity of the asymmetric and symmetric CH_2 stretching bands were determined accordingly (Fig. 11). As shown in Fig. 10, the intensity ratio $I(\nu_{as})/I(\nu_s)$ against temperature shows clearly the existence of the two crystalline forms of the molecule. The intensity ratio starts decreasing continuously up to 45–50 °C where the first melting point occurs according to the results of thermal analysis, and then the intensity ratio increases sharply at 60 °C where a reorganisation of the sample is taking place, followed by a decrease till the melting point of the compound. On the other hand, the band position of ν_s (CH_2) is a sensitive probe for monitoring intramolecular conformational chain disorder concomitantly with intermolecular chain–chain packing disorder. The peak position of

Table 2
Low-frequency Raman bands of 2-amino alcohols

n	LAM-1 (cm^{-1})	LAM-3 (cm^{-1})	Other bands (cm^{-1})
14	48.9 (46.4)	178.0/175.6 (168.0)	22.3, 26.8, 48.9, 132.1
16	41.7 (41.5)	142.5/138.3 (140)	10.5, 13.8, 24.8, 33.0, 120.8
18	39.1 (39.4)	135.5/129.7 (135.5)	19.4, 75.7, 108.7

n, number of carbon chain atoms. Corresponding values for *n*-alcohols are in parentheses (Soutzidou et al., 2002).

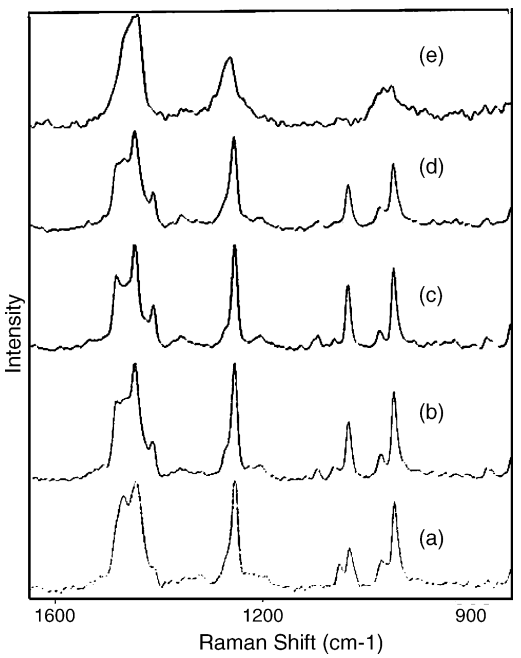

Fig. 9. Raman spectra (850–1650 cm^{-1}) of 2-amino-hexadecanol at different temperatures: (a) 30 °C; (b) 60 °C; (c) 80 °C; (d) 90 °C; (e) 110 °C.

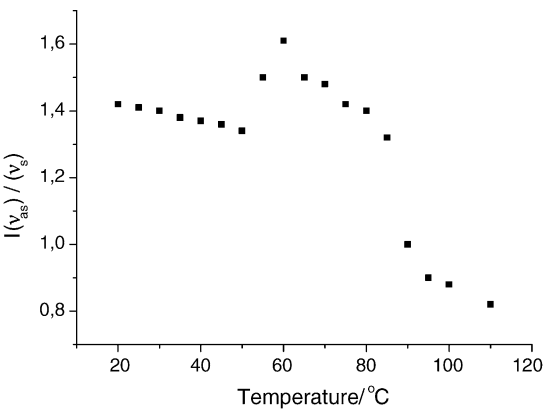

Fig. 10. Temperature dependence of the intensity ratio $I(\nu_{as})/(\nu_s)$ of 2-amino-hexadecanol.

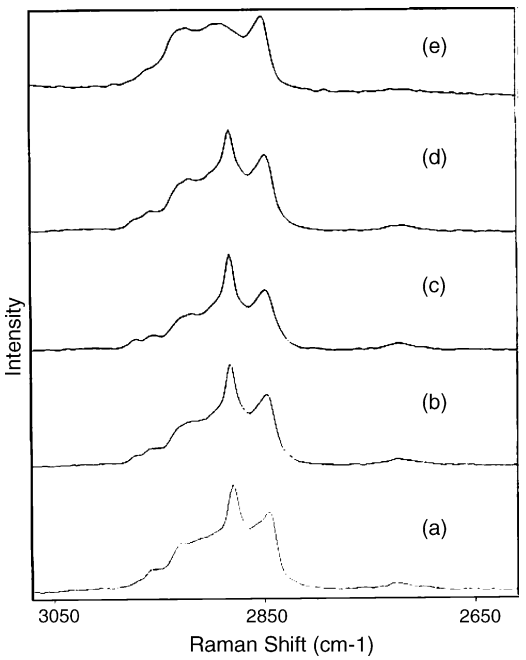

Fig. 11. Raman spectra (2600–3100 cm^{-1}) of 2-amino-hexadecanol at different temperatures: (a) 30 °C; (b) 60 °C; (c) 80 °C; (d) 90 °C; (e) 110 °C.

the symmetric CH_2 stretching mode shifts from 2845 to 2847 cm^{-1} in the course of the melting point of the first crystalline phase followed by a decrease, and then shifts to 2851 cm^{-1} at the melting point of the compound. The points of inflection of the relevant curve coincide approximately with the observed transition temperatures of the DSC curves by taking in consideration the difference between the thermal treatment of the sample by DSC and Raman scattering.

4. Concluding remarks

Different techniques were used in the present work to study the phase transitions of racemic long chain 2-

amino alcohols. Two crystalline phases were observed after re-crystallisation of all 2-amino alcohols that were studied. The first phase melts at a temperature considerably lower followed by a re-organisation of the sample, as shown by the results of DSC and Raman spectroscopy, in comparison to the melting point of the compound. At the rotator phase, the molecular mobility increases as shown by the results of dielectric spectroscopy with no change of the crystal structure of the sample as shown by the results of Raman and dielectric spectroscopy. 2-Amino alcohols molecules are packed in lamellar structures where they crystallise in double layers as shown by the low-frequency Raman results. Finally, a comparison of low-frequency Raman spectra for 2-amino alcohols and the corresponding *n*-alcohols indicates a similarity about the structure of both compounds.

Acknowledgements

This work was partially supported by University of Athens (Grant: 70/4/3355). The authors like to thank Professor G. Kokotos who kindly read the manuscript and made many valuable comments.

References

Amelinckx, S., 1955. Growth features on crystals of long-chain compounds. Acta Crystallogr. 8, 530–537.

Boistelle, R., Simon, B., Pèpe, G., 1976. Polytypic structures of *n*-$C_{28}H_{58}$ (octacosane) and *n*-$C_{36}H_{74}$ (hexatriacontane). Acta Crystallogr. B32, 1240–1243.

Campbell, C., Viras, K., Masters, A.J., Craven, J.R., Hao, Z., Yeates, S.G., Booth, C., 1991. Low-frequency Raman-active modes in α-methyl, ω-hydroxyoligo(oxyethylene)s. J. Chem. Phys. 95, 4467–4651.

Constantinou-Kokotou, V., 2002. Synthesis and biological activities of long chain 2-amino alcohols. Lett. Pept. Sci. 9, 143–150.

Del Olmo, E., Macho, A., Alves, M., Lopez, J.L., el Banoua, F., Munoz, E., San Feliciano, A., 2002. Long-chain aminoalcohol and diamine derivatives induce apoptosis through a caspase-3 dependent pathway. Bioorg. Med. Chem. Lett. 12, 2621–2626.

Denicolo, I., Doucet, J., Craievich, A.F., 1983. X-ray study of the rotator phase of paraffins(III): even-numbered paraffins $C_{18}H_{38}$, $C_{20}H_{42}$, $C_{22}H_{46}$, $C_{24}H_{50}$ and $C_{26}H_{54}$. J. Chem. Phys. 78, 1465–1473.

Donth, E., 2001. The Glass Transition. Springer, Berlin.

Hirose, R., Hamamichi, N., Kitao, Y., Matsuzaki, T., Chiba, K., Fujita, T., 1996. 2-Aminoalcohol immunosuppressants: structure-activity relationships. Bioorg. Med. Chem. Lett. 6, 2647–2650.

Huang, C., Levin, I.W., 1983. Effect of lipid chain length inequivalence on the packing characteristics of bilayer assemblies. Raman spectroscopic study of phospholipid dispersions in the gel state. J. Phys. Chem. 87, 1509–1513.

Kaneko, F., Sakashita, H., Kobayashi, M., Kitagawa, Y., Matsuura, Y., Suzuki, M., 1994. Double-layered polytypic structure of the E form of octadecanoic acid, $C_{18}H_{36}O_2$. Acta Crystallogr. C50, 247–250.

Kobayashi, M., Kobayashi, T., Ito, Y., Chatani, Y., Tadokoro, H., 1980. Another orthorhombic crystal modification of *n*-hexatricontane and its vibrational spectra. J. Chem. Phys. 72, 2024–2031.

Kobayashi, M., Kobayashi, T., Ito, Y., Sato, K., 1984. Polytipism in *n*-fatty acids and low-frequency Raman spectra: stearic acid B form. J. Chem. Phys. 80, 2897–2903.

Kokotos, G., Constantinou-Kokotou, V., Fernadez, E.D., Toth, I., Gibbons, W.A., 1992. Lipidic peptides. 14. Conversion of racemic lipidic amino acids into sphingosine and ceramide analogs and 1,2-diamines. Lieb. Ann. Chem. 961–964.

Kokotos, G., Padron, J.M., Noula, C., Gibbons, W.A., Martin, V.S., 1996. A general approach to the enantiomeric synthesis of lipidic alpha-amino acids, peptides and vicinal amino alcohols. Tetrahedron-Asymmetry 7, 857–866.

Kokotos, G., Constantinou-Kokotou, V., Noula, C., Hadjipavlou-Lithina, D., 1999. Synthetic routes to lipidic diamines and amino alcohols: a class of potential antiinflammatory agents. Lipids 34, 307–311.

Kremer, F., Schoenhals, A. (Eds.), 2002. Broadband Dielectric Spectroscopy. Springer, Berlin.

Magrioti, V., Hadjipavlou-Litina, D., Constantinou-Kokotou, V., 2003. Synthesis and in vivo anti-inflammatory activity of long-chain 2-amino-alcohols. Bioorg. Med. Chem. Lett. 13, 375–377.

Markidis, T., Padron, J.M., Martin, V.S., Peters, G.J., Kokotos, G., 2001. Synthesis and in vitro cytotoxicity of long chain 2-amino alcohols and 1,2-diamines. Anticancer Res. 21, 2835–2839.

Mijovic, J., Sy, J.-W., 2002. Molecular dynamics during crystallisation of poly(L-lactic acid) as studied by broad-band dielectric relaxation spectroscopy. Macromolecules 35, 6370–6376.

Minoni, G., Zerbi, G., 1982. End effects on longitudinal accordion modes: fatty acids and layered systems. J. Phys. Chem. 86, 4791–4798.

Nagle, J.F., 1980. Theory of the main lipid bilayer phase transition. Ann. Rev. Phys. Chem. 31, 157–195.

Nikonorova, N., Borisova, T., Barmatov, E., Pissis, P., Diaz-Calleja, R., 2003. Dielectric relaxation and thermally stimulated discharge currents in liquid – crystalline side – chain polymethacrylates with phenylbenzoate mesogens having tail groups of different length. Macromolecules 36, 5784–5791.

O'Leary, T.J., Ross, P.D., Levin, I.W., 1984. Effects of anesthetic and nonanesthetic steroids on dipalmitoylphosphatidylcholine liposomes: a calorimetric and Raman spectroscopic investigation. Biochemistry 23, 4636–4641.

Snyder, R.G., Strauss, H.L., Alamo, R., Mandelkern, L., 1994. Chain-length dependence of interlayer interaction in crystalline *n*-alkanes from Raman longitudinal acoustic modes measurements. J. Chem. Phys. 100, 5422–5431.

Soutzidou, M., Masters, A.J., Viras, K., Booth, C., 1999. The LAM-1 band in the low-frequency Raman spectra of even and odd mono-substituted *n*-alkanes. Phys. Chem. Chem. Phys. 1, 415–419.

Soutzidou, M., Glezakou, V.A., Viras, K., Helliwell, M., Masters, A.J., Vincent, M.A., 2002. Low-frequency Raman spectroscpopy of *n*-alcohols. LAM vibration and crystal structure. J. Chem. Phys. B 106, 4405–4411.

Sprunt, J.C., Jayasooriya, U.A., Wilson, R.H., 2000. A similtaneous FT-Raman–DSC (SRD) study of polymorphism in s*n*-1,3-distearoyl-2-oleoylglycerol (SOS). Phys. Chem. Chem. Phys. 2, 4299–4305.

Ungar, G., 1983. Structure of rotator phase in *n*-alkanes. J. Phys. Chem. 87, 689–694.

Viras, K., Viras, F., Campbell, King, T.A., Booth, C., 1989. Low-frequency Raman spectra of even α,ω-disubstituted *n*-alkanes. J. Phys. Chem. 93, 3479–3483.

Wunderlich, B., 1990. Thermal Analysis. Academic Press, London.